Iranian Journal of Materials Forming 10 (2) (2023) 44-54

IJMF

Online ISSN: 2383-0042

Iranian Journal of Materials Forming

Journal Homepage: http://ijmf.shirazu.ac.ir

Research Article

Using JMatPro Simulation to Study the Effect of Heat Treatment Temperature on the Dissolution of Gamma-Prime Phase in Inconel 617 Nickel-Based Superalloy

E. Asghari[1], R. Hayati[1*], A. Momeni[2], N. Setoudeh[1] and A. Mohassel[1]

[1] Department of Materials Engineering, Faculty of Engineering, Yasouj University, Yasouj, Iran
[2] Department of Materials Engineering, Faculty of Engineering, Hamedan University of Technology, Hamedan, Iran

ARTICLE INFO

Article history:

Received 3 June 2023
Reviewed 1 July 2023
Revised 17 July 2023
Accepted 18 July 2023

Keywords:

Inconel 617
Gamma-prime
JMatPro
Heat treatment
Microstructure

Please cite this article as:

E. Asghari, R. Hayati, A. Momeni, N. Setoudeh, A. Mohassel, Using JMatPro simulation to study the effect of heat treatment temperature on the dissolution of gamma-prime phase in Inconel 617 nickel-based superalloy, *Iranian Journal of Materials Forming*, 10(2) (2023) 44-54.

ABSTRACT

In this study the effect of heat treatment temperature on the formation and dissolution of gamma-prime phase has been studied in Inconel 617. Since the working temperature of Inconel 617 is above 540°C, the samples were heat treated at different temperatures in a range between 550 to 850°C and simulations were performed at the same temperatures by the JMatPro software. It was found that the gamma-prime phase with different percentages (below 10%) would exist in the temperature range of 550 to 800°C. However, it would gradually decrease as the temperature increases and finally dissolve completely at temperatures over 800°C. The observations by metallography were in good agreement with the predictions made by the JMatPro software. The microstructure investigations using the optical and field emission electron microscopy showed that the gamma-prime phase exists at 650°C and 750°C, but its weight percent decreases with increasing temperature, so that at 850°C no gamma-prime can be detected.

1. Introduction

Superalloys are unique in terms of high temperature mechanical properties and environmental resistance, which are generally used at temperatures above 540°C and are the first choice for structural applications at high temperatures. Although ceramics have very high environmental resistance, their low fracture toughness limits the use of these materials in structural applications. Additionally, refractory metal alloys can maintain their mechanical properties at high temperatures due to their high melting temperature, but these materials have poor oxidation resistance. Superalloys having a combination of environmental

* Corresponding author
E-mail address: r.hayati@yu.ac.ir (R. Hayati)
https://doi.org/10.22099/IJMF.2023.47549.1260

resistance and high mechanical properties at high temperatures are superior to other alloy systems and have attracted a considerable attention in recent years [1].

Based on the main alloying elements in their composition, superalloys are classified into three categories: nickel-based, cobalt-based, and iron-based. The entire family of superalloys have a basic FCC structure along with a number of secondary strengthening phases. Nickel-based superalloys are creep-resistant materials that are used in high temperature conditions. Additionally, they are most widely used in aviation and gas turbine industries due to their high corrosion and oxidation resistance. To improve the oxidation resistance, enough Al is added to form the Al_2O_3 oxide layer, and in order to increase the oxidation resistance, Cr is added to form the outer surface of the Cr_2O_3 alloy. Accordingly, Ni-based superalloys are used in the gas turbine combustion chambers, channels and transmission lines for the petrochemical process, heat treatment equipment and in nitric acid production. Nickel-based superalloys have reached the highest level of temperature/strength combination, so they are ideal for tough applications such as turbine blades. As mentioned, superalloys are generally suitable for working at temperatures above 540°C and below the melting point, which is usually 1204°C [2-4].

Ni-based superalloys have the γ phase as the matrix with an austenitic FCC lattice and various secondary phases also exist. These secondary phases are: 1-FCC carbides of M_7C_3, M_6C, $M_{23}C_6$, MC type, 2-γ' phase with FCC crystal structure and $Ni_3(Ti, AL)$ composition, 3-γ'' phase with BCT crystal structure and Nb_3Ni composition, 4-η phase with HCP crystal structure and Ni_3Ti composition, 5-δ intermetallic phase with orthorhombic crystal structure and Ni_3Nb composition. Detrimental phases are also formed in superalloys. Among these phases, σ, μ and Laves phases can be mentioned. These phases have a close-packed tetragonal (TCP) structure which are ignored if they are minor, but in larger amounts their harmful effect should be considered [3].

Considering the importance of the Inconel 617 superalloy in high temperature applications, a considerable amount of research has been carried out in recent years. In these studies, the effect of different heat treatment processes on the existence of beneficial/detrimental phases and the corresponding mechanical properties were investigated [5-6].

Different computer software has been used to model and simulate the materials properties such as thermodynamic-based physical properties [7]. Some researchers have used the software to estimate the final properties of alloys by applying the properties of the individual constituents and interrelating the microstructure to the physical properties [8-9]. JMatPro (**J**ava **Mat**erials **Pro**perties) is a computer software which has been widely used to model the thermodynamic, mechanical and thermo-physical properties of metals and alloys [10-11]. JMatPro is a simulation software which calculates a wide range of the materials properties for alloys and is particularly aimed at multi-component alloys used in industrial practice. This software emphasizes the calculation methods that are based on sound physical principles rather than purely statistical methods. In this way, many of the shortcomings of methods such as regression analysis are overcome. The inclusion of microstructurally sensitive parameters means that it is possible to make the link with material models that are currently being developed for the prediction of microstructure [12].

Unlike other software, it is designed based on physical principals, not merely statistical [7]. Regarding the Ni-based superalloys, in several publications this software was used to calculate the linear expansion of this alloy at different temperatures and the results were compared with experimental data [13]. Saunders et al. have reported a brief review on the application of JMatPro in multi-phase superalloys including Ni-based ones [14]. According to this paper, JMatPro software is capable of predicting the mechanical properties such as the strengthening behavior of gamma and gamma-prime phases in Ni-based superalloys [7]. Miodownik, et al. simulated the secondary creep behavior of commercial and solid solution superalloys and compared the results with experimental data [15]. Coarsening of gamma-prime phase at high annealing temperatures is a demanding feature in Ni-based superalloys. Li et al. investigated the coarsening rate of γ' in Ni-based and Ni-Al superalloys and compared them with the calculated results of CALPHAD software. They reported interesting results for commercial Ni-Al based alloys. In all temperature ranges excluding the low temperatures, they showed superior agreement between experimental and calculated results, which was attributed to the lower lattice misfit in commercial alloys [16].

Sani et al. studied the behavior of Co-based superalloy prepared with the casting method. They predicted the formation temperature of different phases with JMatPro software and compared it with experimental results. They concluded that the Ti and W-rich matrix phase (gamma) was strengthened with gamma-prime. In addition to the carbide and gamma-prime phases, the thermodynamically stable μ phase, must exist in the alloy matrix. Finally, their comparison showed that the software predicted the phases of the cast alloy accurately and they were consistent with the experimental data [17]. In another study, thermodynamic calculations were used to investigate the effect of annealing treatment on the microstructure and phase formation of IN738LC superalloy. It was found that the equilibrium deposits of the gamma-prime phase are formed at annealing temperatures of about 1130°C, and at higher temperatures they are not stable. Additionally, $M_{23}C_6$ carbides are thermodynamically stable at temperatures below 1000°C. Their results revealed that that JMatPro software is eligible to predict the formation and dissolution of phases in IN738LC nickel base superalloys [18].

In this paper, the commercial Ni-based superalloy, Inconel 617, was heat treated at different temperatures and the gamma-prime phase dissolution was studied by microscopical examinations. Additionally, JMatPro software was used to calculate the gamma-prime phase at different annealing temperatures and the results were compared with the laboratory investigations.

2. Experimental Procedure

In this project, the Inconel 617 alloy with chemical composition according to Table 1 was investigated. Annealing treatments were carried out on the samples with the dimensions of 10 mm×15 mm at temperatures of 650, 750 and 850°C for 30 min. The annealed samples were then immediately quenched in water to the ambient temperature.

Table 1. Chemical composition of Inconel 617 used in this investigation (values in wt.%).

Chemical Composition (wt.%)					
Ni	**C**	**Si**	**Mn**	**P**	**S**
55.50	0.054	0.10	0.11	0.006	0.001
Cr	**Mo**	**Fe**	**W**	**V**	**Al**
20.96	8.02	1.35	0.20	0.02	1.22
Co	**Cu**	**Nb**	**Sn**	**Ta**	**Ti**
11.97	0.043	0.027	0.0005	0.037	0.33
Zn	**As**	**Zr**	**Mg**	**B**	
0.003	0.002	0.004	0.017	0.001	

To reveal the initial microstructure, the surface of the samples was prepared with the standard metallographic techniques. After mechanical polishing using the diamond paste, samples were etched in a reagent composed of $HCl:HNO_3$ equal to 3:1, and then washed out with ethanol. The microstructure was observed and analyzed with an optical microscope (NeoPhot-32, Germany). To investigate the phase structure and the composition, X-ray diffraction (XRD) analysis was used (D8-Advance machine, Bruker, Germany). To perform EDS analyses, field emission scanning electron microscope (FESEM) (model EM-8000, KYKY company, China) was used and the atomic percentage of elements in different phases were determined.

The microstructure simulation was carried out by the JMatPro software (England, Version 7.0.0). Using the software, the amount of the gamma-prime phase in the temperature range of 650 to 850°C was calculated and the approximate dissolution temperature of this phase was predicted. The results of quantometer analysis (percentage of alloy elements) were imported into the JMatPro software and the appropriate temperature range was selected. In the following, the value of the different phases was calculated and the corresponding graphs of the weight percentage versus temperature are designed. To better display the gamma-prime status in the temperature range of 650 to 850°C, the three-dimensional diagram of the constituent phases of Inconel 617 alloy including the gamma-prime phase was designed and the values were predicted at different temperatures. It should be noted that other strengthening phases existing in the alloy are not considered in the results of this study.

3. Results and Discussion

The optical micrograph of the cross-sectional surface of the as-received sample after polishing and before etching has been shown in Fig. 1. As revealed, some nitride inclusions can be observed as a result of previous deformation processes, also reported in previous studies [19]. To better clarify the nature of cuboid phases, EDS analysis was performed and the results are discussed in the next sections. The microstructure of the as-received specimen is illustrated in Fig. 2. The matrix shown in Fig. 2(a) evidently consisted of equiaxed gamma grains, which mostly contain annealing twin bands. A large number of inclusions, observed in Fig. 1, were also detected in the grains and grain boundaries in Figs. 2(a), 2(b) and 2(c). The magnified image in Fig. 2(d) showed that the as-received microstructure contains very small gamma-prime particles formed inside the gamma grains.

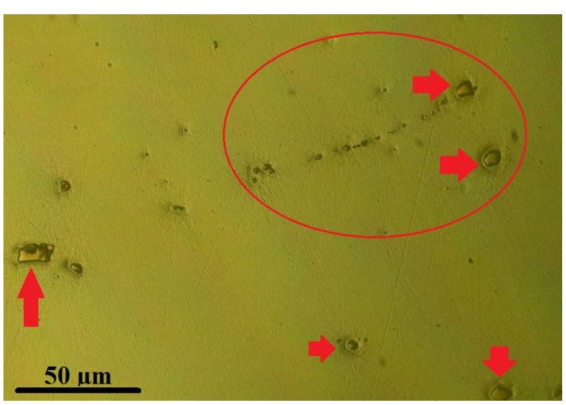

Fig. 1. Optical microscope image from the polished surface of the initial sample, the cuboid inclusions are marked by arrows.

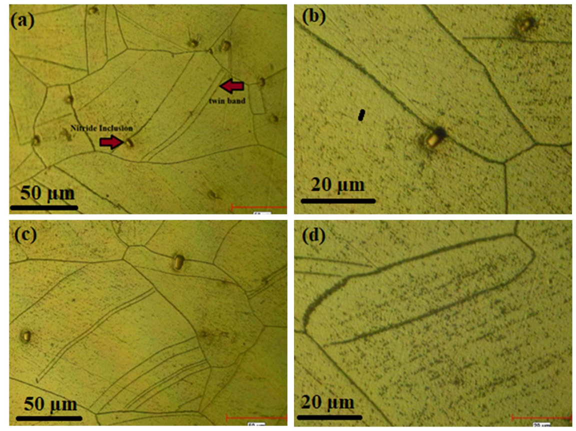

Fig. 2. Optical microscopy micrographs of the as-received Inconel 617 superalloy sample: (a) the equiaxed gamma grains, (b) TiN inclusions, (c) twin bands inside the grains, and (d) magnified image showing the distribution of gamma prime particles.

In order to further study the constituent phases of the initial sample, XRD analysis was carried out and the pattern, shown in Fig. 3, was investigated with the Xpert High Score software. The XRD pattern is matched with Ni base metal that have FCC crystal structure and JPCPDS No. 96-901-3034. The sharpest peak at 2θ=43.74° is labeled with gamma matrix, gamma-prime and nitride/carbide phases. The FCC crystal structure of gamma-prime phase, Ti_4Ni_{12} with JPCPDS No. 96-101-0453 is similar to the matrix with a slight difference in its lattice parameters. The smallest peak at 2θ=50.92° is attributed to gamma matrix and gamma-prime

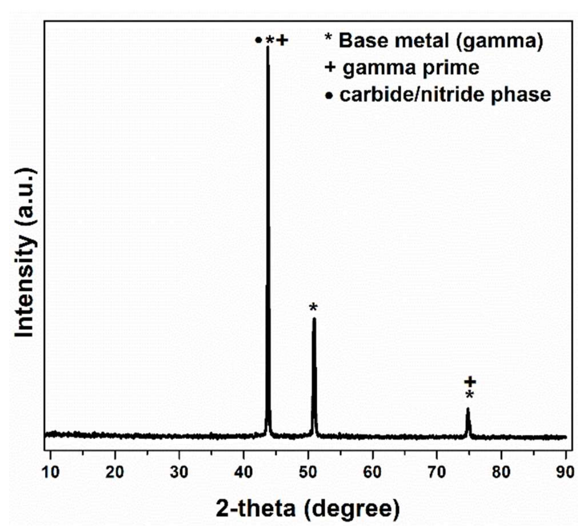

Fig. 3. XRD pattern of the as-received Inconel 617 sample.

strengthening phase. It should be noted that, although at 2θ=43.74° the main peak of Ni is overlapped with a small peak of tetragonal Ti_8N_4 (96-110-0030); the amount of nitride/carbide phases would be negligible. These results are in good agreement with previous studies [20].

To study the microstructure with further details, the as-received sample was examined by FESEM, as shown in Fig. 4. In agreement with the observations in Fig. 2, the FESEM micrographs confirm that the microstructure includes gamma matrix with gamma-prime interior particles and some nearly cuboidal inclusions. Based on the chemical composition given in Table 1, their shape proposes that they may be Ti(C,N). As mentioned in the literature, the carbonitride phase does not deteriorate the mechanical properties of Ni-based super alloys [18-19]. According to Fig. 4(b), the size of gamma-prime particles appears to be below 50 nm, while the inclusions are as large as 5-7 microns.

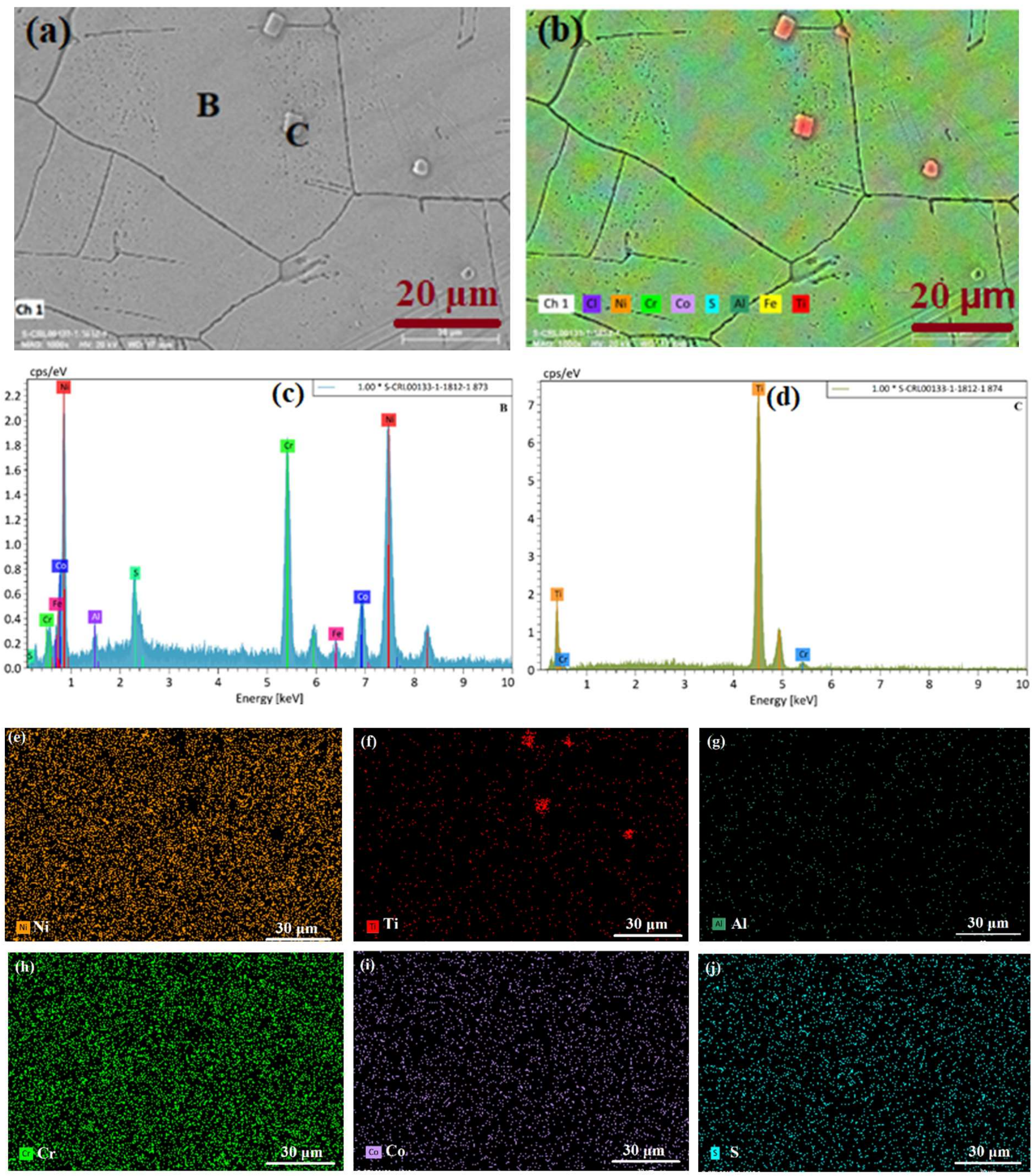

Fig. 4. FESEM image and the corresponding map showing the microstructure and elemental analysis of as-received Inconel 617 with two points marked as B and C for EDS analysis, (c) and (d) EDS spectra of points B and C in (a), (e)-(j) the elemental analysis of map of Fig. 4(b).

EDS analysis performed on the matrix and inclusions have been presented in Fig. 4. According to the results, point B that is the grain insider region is mainly composed of the basic alloying elements, i.e. Ni, Cr, Co, and Al, while other alloying elements, i.e. Ti, W, and Mo are absent (Table 2). As these elements are more active than others, it appears that we should find them in some compounds, like carbides or inclusions. According to Fig. 4(c) and the elemental analysis in Table 2, point C is rich in titanium, but the density of chromium atoms is not significant in these regions. Considering that there is no tendency for the formation of intermetallic phase between Ti and Cr in the Ni-based superalloys, it is possible to say that the device has recognized chromium by mistake. Additionally, due to the proximity of nitrogen and chromium peaks, the phase can be distinguished as titanium nitride (TiN). Nitrides have a high melting point and generally remain in the structure of superalloys and do not undergo dissolution even in the molten alloy [22]. The cuboidal morphology of TiN, which has been also reported in the literature [21], shows that it forms nearly coherent interfaces with the gamma matrix of the alloy.

Table 2. EDS analysis results of points B and C in Fig. 4(a) (values are in at.%)

Point	Ni	Cr	Co	S	Al	Fe	Ti
B	55.12	23.17	11.70	5.45	2.90	1.66	-
C	-	2.44	-	-	-	-	97.56

Fig. 5 shows the microstructural/chemical simulation of the studied alloy via the JMatPro software. The simulation results revealed that in the desired temperature range (650 to 850°C), the weight fraction of gamma phase gradually increases from about 85% to 100%. On the other hand, the initial amount of gamma-prime phase, that is about 5 wt.% at 650°C, gradually decreases by increasing the temperature and it completely dissolves at about 804°C.

Fig. 6 displays the variation in the contents of sub-phases, i.e. gamma-prime, carbides and sigma, in the temperature range of 650 to 850°C. According to the results summarized in Table 3, all the sub-phases are dissolved into the matrix and a single-phase gamma microstructure is obtained at temperatures over 800°C. Hence, annealing at 850°C can be an appropriate solution of heat treatment for Inconel 617 and any temperature range higher than 850°C can be used as the optimal hot working temperature range for the alloy.

In order to verify the simulation results, the samples were heat treated at different annealing temperatures of 650, 750 and 850°C for 30 min. The microstructure of the annealed samples was examined with an optical microscopy and the results are demonstrated in Fig. 7.

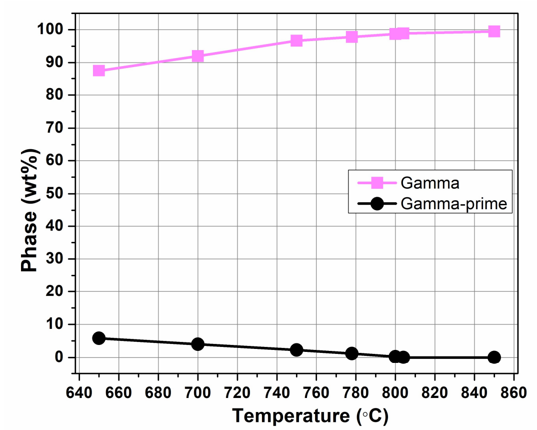

Fig. 5. Variation in the weight percent of gamma and gamma-prime phases in the temperature range of 650 to 850°C, predicted by JMatPro software.

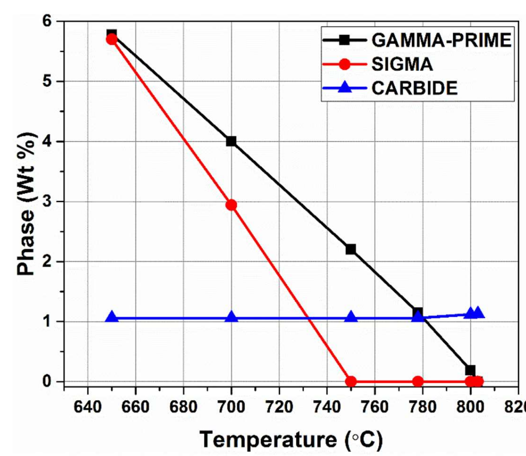

Fig. 6. Variation in the content of sub-phases, gamma-prime, carbides and sigma in the as-received sample of Inconel 617 superalloy at different temperatures, predicted by JMatPro software.

Table 3. Weight percentage of sub-phases in Inconel 617 at different temperatures

Temperature (°C)	650	700	750	778	800	804
Gamma-prime (wt.%)	5.78	4.00	2.25	1.15	0.19	0
Sigma (wt.%)	5.7	2.94	-	-	-	-
Carbide (wt.%)	1.06	1.06	1.06	1.06	1.12	1.13

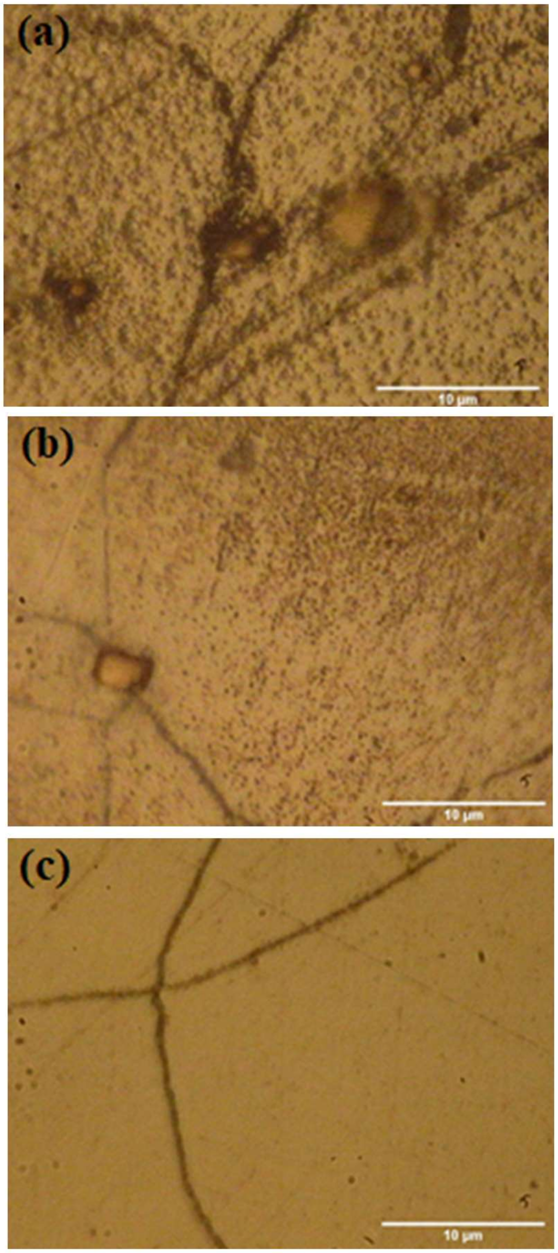

Fig. 7. Optical microscopy photographs showing the microstructure of Inconel 617 superalloy samples annealed at (a) 650°C, (b) 750°C, and (c) 800°C.

While after annealing at 650 °C (Fig. 7(a)), a large number of fine gamma-prime particles could be observed, after annealing at 750°C (Fig. 7(b)), the amount of gamma-primes considerably decreased. In agreement with the predictions made by the JMatPro software in Figs. 5 and 6, Fig. 7(c) confirms that after annealing at 850°C, the gamma-prime phase has been totally dissolved in the matrix. This is also the case for other sub-phases such as carbides and sigma.

The sample annealed at 650°C was further analyzed by FESEM and the results are demonstrated in Fig. 8. It's the magnified view of which clearly shows the distribution of fine gamma-prime particles inside the gamma grains. The EDS analyses of points marked by A and B in Fig. 8(b) have been presented in Figs. 8(b) and 8(c). The chemical analyses summarized in Table 4 clearly indicates that the gamma-prime phase exists at this temperature and is mainly concentrated at grain boundaries (point B), which complies with $Ni_3(Al,Ti)$. Additionally, the region marked as A seems to be the solid solution of the alloying elements of Ni matrix, rich in iron and cobalt. Based on the JMatPro predictions and the results of EDS analysis at points A and B, it is concluded that a sigma phase with chemical composition $(Cr,Mo)_x(Ni,Co)_y$ (x and y:1-7) may also exist in the gamma matrix [23].

The FESEM examinations of the samples heat treated at 750 and 800°C are illustrated in Figs. 9 and 10. Fig. 9(a) clearly indicates that gamma-prime still exists in the sample annealed at 750°C; but its percentage has remarkably decreased compared to the temperature of 650°C. The chemical analysis of points marked as A and B in Fig. 9(b), summarized in Table 5, indicates that point B is richer in Al and Ti than point A. Hence, it is confirmed that the particles in Fig. 9(b) are in the gamma-prime phase.

The FESEM images shown in Figs. 10(a)-10(k) clearly revealed that the gamma-prime phase has been completely dissolved after annealing at 850°C. It should be noted that quenching has been able to effectively suppress the formation of gamma-prime after annealing and therefore formation of new gamma-prime inside the gamma matrix needs a new cycle of aging at temperatures below 800°C. These results are also consistent with the predictions made by the JMatPro software. The chemical analysis of points A and B summarized in Table 6 indicate that there is no remarkable difference between the chemical compositions inside the grains and grain boundaries, therefore, annealing at 850°C leads to a homogeneous distribution of all alloying elements in the alloy.

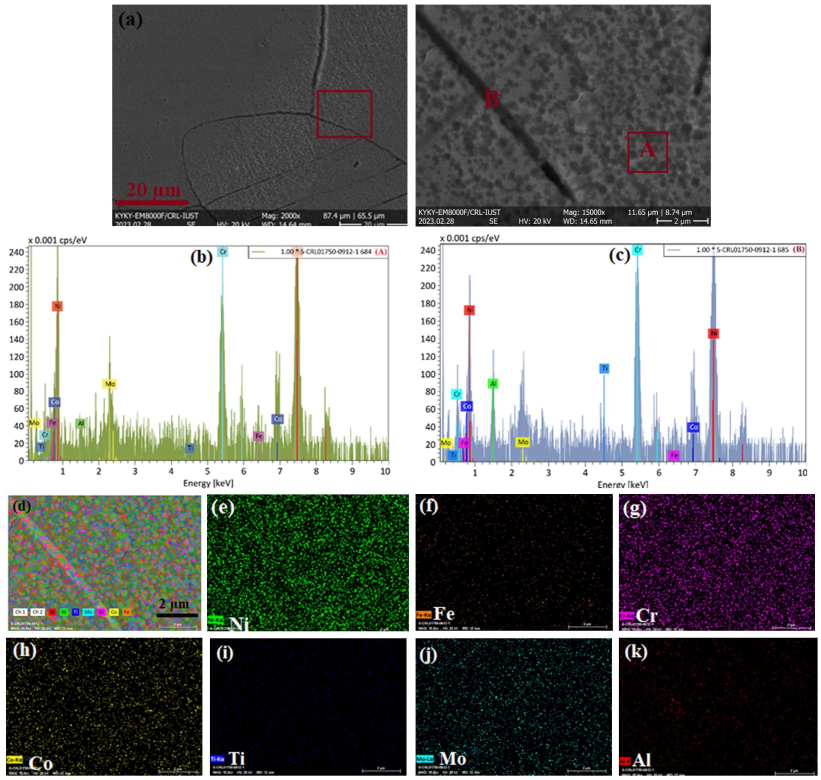

Fig. 8. (a) FESEM micrographs and (b) and (c) the corresponding EDS spectra from the regions marked as A and B in (a), (d) to (k) EDS mapping of (a). All the analysis has been performed on the sample annealed at 650°C.

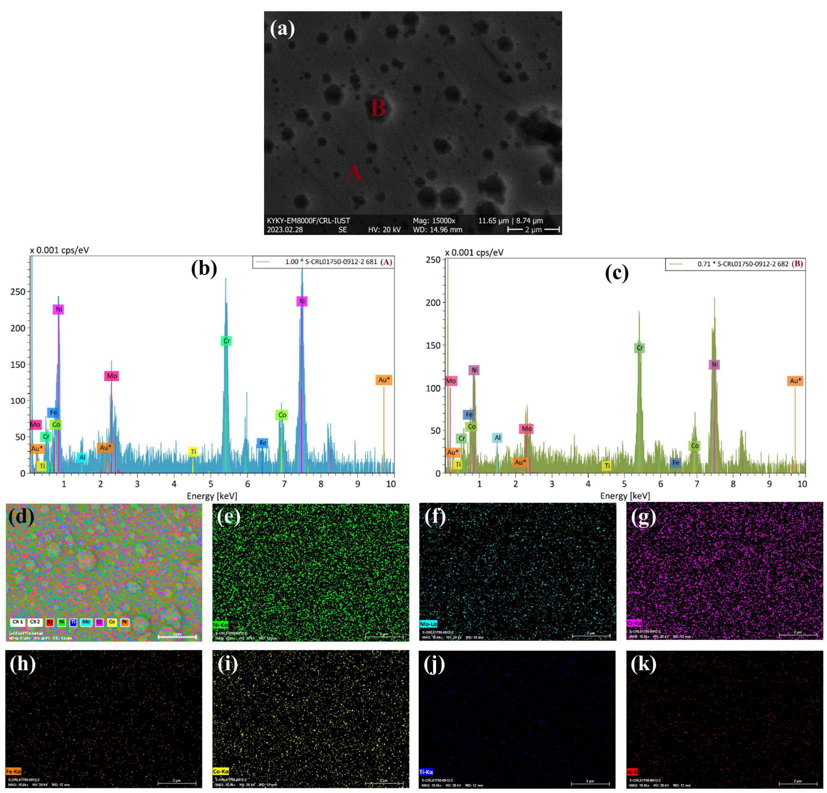

Fig. 9. (a)FESEM micrographs and (b) and (c) EDS spectra of points marked as A and B in (a) and (d) to (k) EDS mapping from (a). All the analysis has been performed on the sample annealed at 750°C.

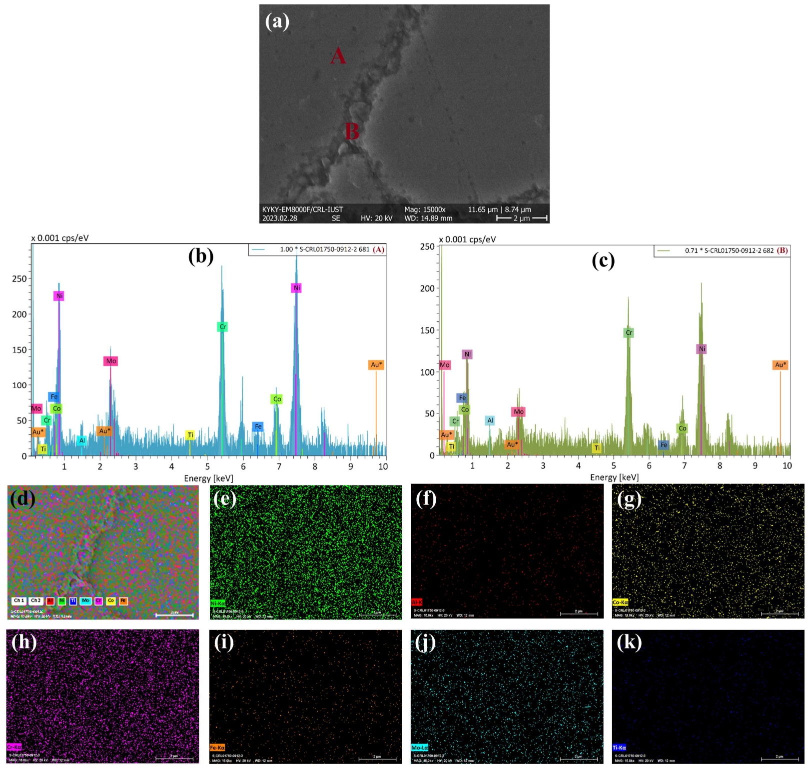

Fig. 10. (a) FESEM micrographs and (b) and (c) EDS spectra of points marked as A and B in (a) and (d) to (k) EDS mapping from (a). All the analysis has been performed on the sample annealed at 850°C.

Table 4. Chemical composition of points marked as A and B in Fig. 8 (EDS analysis of Inconel 617 superalloy samples annealed at 650, values are in at.%)

Point	Ni	Cr	Co	Mo	Fe	Al	Ti
A	57.08	21.09	12.17	4.43	2.75	2.20	0.31
B	44.03	27.11	8.74	4.55	0.67	7.31	0.29

Table 5. Chemical composition of points marked as A and B in Fig. 9 (values are in at.%)

Point	Ni	Cr	Co	Mo	Fe	Al	Ti
A	51.28	27.87	10.94	5.91	1.76	2.14	0.10
B	54.64	23.57	6.44	8.84	0.73	4.59	1.18

Table 6. Chemical composition of points marked as A and B in Fig. 10 (values are in at.%)

Point	Ni	Cr	Co	Mo	Fe	Al	Ti	C
A	43.63	25.54	8.46	4.35	1.00	1.78	-	16.24
B	45.82	24.34	9.53	3.54	0.89	1.59	-	14.3

4. Conclusion

In this study the effect of heat treatment at temperatures in a range of 650-850°C on the microstructure and phases in Inconel 617 superalloy were studied and the results were compared with the predictions by the JMatPro software. The major results of this research can be drawn as follows:

1. The JMatPro software satisfactorily predicts the microstructural changes and the contents of gamma and gamma-prime at different annealing temperatures. The accuracy of the predictions of the software were verified by the experimental heat treatments.
2. In the temperature range of 650 to 850°C, the amount of gamma-prime phase is reduced by increasing temperature. The weight percentage of gamma-prime does not proceed 6 wt.% in this

temperature range.

3. The dissolution temperature of the gamma-prime phase is estimated to be approximately 805°C and at temperatures in the range of 805-850°C the gamma-prime phase is completely dissolved in the gamma matrix.

Conflict of Interests

The authors declare that they have no known competing financial interests or personal relationships that could have appeared to influence this paper.

Funding

The authors would acknowledge the research council of Yasouj University for their financial supports.

5. References

[1] M.J. Donachie, S.J. Donachie, Superalloys: a technical guide, ASM International, 2002, pp.1-9.

[2] K. Park, P. Withey, Compositions of gamma and gamma prime phases in an as-cast nickel-based single crystal superalloy turbine blade, *Crystals*, 12(2) (2022) 299.

[3] M. Durand-Charre, The microstructure of superalloys, Gordon and Breach, Amsterdam, 1997.

[4] S. Bagui, B.P. Sahu, K. Laha, S. Tarafder, R. Mitra, Creep deformation behavior of Inconel 617 alloy in the temperature range of 650 C to 800 C, *Metallurgical and Materials Transactions A*, 52 (2021) 94-107.

[5] Sh. Li, P. Liu, J. Song, W. Guo, J. Xiong, J. Li, Microstructural characteristics and mechanical response of diffusion bonding Inconel 617 superalloy, *Journal of Alloys and Compounds*, 953 (2023) 169899.

[6] Y. Wei, S. Yang, H. Xu, X. Ling, Experimental characterization of flat indentation creep behavior of Inconel 617, *Vacuum*, 208 (2023) 111715.

[7] N. Saunders, A.P. Miodownik, CALPHAD (calculation of phase diagrams): a comprehensive guide, Elsevier, 1998.

[8] Z. Fan, P. Tsakiropoulos, A.P. Midownik, A generalized law of mixtures, *Journal of Materials Science*, 29 (1994) 141-150.

[9] Z. Fan, A microstructural approach to the effective transport properties of multiphase composites, *Philosophical Magazine A*, 73(6) (1996) 1663-1684.

[10] N. Saunders, X. Li, A. P. Miodownik, J. P. Schille, An integrated approach to the calculation of materials properties for Ti-alloys, In Titanium-2003. Science and Technology: Proceedings of the 10th World conference on Titanium, Hamburg, Germany, 2003.

[11] N. Saunders, Z. Guo, X. Li, A.P. Miodownik, J.P. Schillé, The calculation of TTT and CCT diagrams for general steels, JMatPro Software Literature, 2004, pp. 1-12.

[12] N. Saunders, Z. Guo, X. Li, A.P. Miodownik, J.Ph. Schillé, Using JMatPro to model materials properties and behavior, JOM, 55 (2003) 60-65.

[13] H. Leggett, J.L. Cook, D.E. Schwab, C.T. Powers, U.S. Air Force Report, AFML-TR-65-147, 1965.

[14] P. Miodownik, J.P. Schille, N. Saunders, Z. Guo, X. Li, Modelling the materials properties and behaviour of Ni-based superalloys, *Superalloys*, 2004, 849-858.

[15] A. Strang, R.D. Conroy, W.M. Banks, M. Blackler, J. Leggett, G.M. McColvin, S. Simpson, M. Smith, Parsons, Engineering issues in turbine machinery, Power Plant and Renewables: Proceedings of the Sixth International Charles Parsons Turbine Conference, Trinity College Dublin, Ireland, Maney. 2003.

[16] N. Saunders, X. Li, A.P. Miodownik, J.P. Schillé, Computer modelling of materials properties, *Materials design approaches and experiences*, 185-197, 2001

[17] S. Aliakbari Sani, H. Arabi, S. Kheirandish, G. Ebrahimi, An investigation the present phases in a cast Co-Al-W Cobalt-base superalloy using experimental methods and JMatPro Software, *Founding Research Journal*, 2(1) (2018) 27-37.

[18] F. Forghani, M. Mehdizade, M. Rayatpoor, Tracing the creep lifetime degradation of IN738LC superalloy based on the primary carbide decomposition reaction and composition changes in the carbide regions, *Journal of New Materials*, 11(42) (2021) 81-94.

[19] Y. Wang, Q. Liu, Z. Cai, H. Wang, L. Shi, K. Li, Nitride precipitation and formation in IN617 superalloy during creep, *Journal of Alloys and Compounds*, 948 (2023) 169709.

[20] S. Basak, S.K. Sharma, K.K. Sahu, S. Gollapudi, J.D. Majumdar, Surface modification of structural material for nuclear applications by electron beam melting: enhancement of microstructural and corrosion properties of Inconel 617, *SN Applied Sciences*, 1 (2019) 1-12.

[21] G.P. Sabol, R. Stickler, Microstructure of nickel-based superalloys, *Physica Status Solidi*, 35(1) (1969) 11-52.

[22] V. Bhanu, D. Fydrych, A. Gupta, C. Pandey, Study on microstructure and mechanical properties of laser welded dissimilar joint of P91 steel and INCOLOY 800HT nickel alloy, *Materials*, 14(19) (2021) 5876.

[23] S. Jeon, H. Lee, I. Jo, D. Shin, K.S. Lee, Degradation of TiN coatings on Inconel 617 and silicon wafer substrates under pulsed laser ablation, *Journal of Materials Engineering and Performance*, 23(5) (2014) 1651-1655.